Hindawi
Mathematical Problems in Engineering
Volume 2021, Article ID 2304796, 16 pages
https://doi.org/10.1155/2021/2304796

Research Article

A Sustainable Design Strategy Based on Building Morphology to Improve the Microclimate of University Campuses in Cold Regions of China Using an Optimization Algorithm

Shuo Chen,[1] **Peng Cui**,[2] **and Hongyuan Mei**[3]

[1]*Faculty of Architecture, Civil and Transportation Engineering, Beijing University of Technology, No. 100 Ping Leyuan Street, Chaoyang District, Beijing 100124, China*
[2]*School of Landscape, Northeast Forestry University, Harbin, 150040, China*
[3]*School of Architecture, Harbin Institute of Technology, Heilongjiang Cold Region Architectural Science Key Laboratory, No. 66 Xidazhi Street, Nangang District, Harbin 15001, China*

Correspondence should be addressed to Shuo Chen; chens@bjut.edu.cn

Received 29 July 2020; Revised 26 April 2021; Accepted 13 May 2021; Published 8 June 2021

Academic Editor: Fausto Arpino

The microclimate affects the quality and efficiency of outdoor spaces of campuses, especially in the cold regions of China. In this paper, we propose a multiobjective optimization method to improve the thermal comfort of the outdoor environment of university campuses in severe cold regions. We used morphology data from 41 universities in the cold region of China to create a layout prototype of a campus cluster. Multiobjective optimization was used, and the effects of sunlight, solar radiation, and wind on the outdoor thermal comfort in winter were considered. A parameterized platform was established for the multiobjective optimization of the microclimate of the simplified model of the campus. A multiobjective optimization based on an evolutionary algorithm was used to obtain 108 groups of nondominated solutions. The optimum outdoor microclimate of the campus was obtained at a building density of 0.21–0.23, a plot ratio of 1.51–1.88, and a road width of 11–14 m. We recommend that buildings are designed based on the wind direction in winter and that the space between buildings is increased.

1. Introduction

The microclimate affects the quality and efficiency of open spaces on university campuses [1] and can be significantly improved by appropriate planning [2–4]. In severe cold regions, the thermal comfort of outdoor spaces on campuses is affected by multiple climatic factors, such as sunlight, solar radiation, and wind speed. Faulty planning can reduce the thermal comfort of the users. Therefore, in this study, we consider the relationship between several climatic factors and the layout of the university campus and propose a design strategy for campuses to optimize the outdoor microclimate. The strategy improves the use efficiency of campus open spaces in cold regions and promotes the sustainable development of the campus environment.

Extensive research has been conducted on the microclimate of urban blocks and street canyons [5, 6]. The users' behavior at universities is similar to people in urban areas; however, the layout of a campus differs from that of urban blocks. The campus layout is characterized by many open spaces and large building clusters. The spatial morphology of the university campus influences the microclimate of the campus [7, 8], and architectural clusters have the greatest influence on the duration of direct solar radiation and the mean radiation temperature [9]. Unlike outdoor spaces on campuses, enclosed areas have good performance for reducing the heating energy consumption and enhancing natural ventilation and cooling [10]. Moreover, the structures on campuses have a significant impact on outdoor solar radiation and wind [11]. A study of university

campuses in cold regions has shown that when the outdoor thermal comfort and heat dissipation of buildings in summer is considered in the design, the time when the outdoor temperature is perceived as uncomfortable is reduced by 25%, and the heat dissipation is reduced by 5% [12]. The main factors affecting the outdoor microclimate include sunlight, temperature, humidity, wind speed, surface material, and the sky view factor [13–15].

The urban climate map (UCM) system is a method to analyze the relationship between urban climate and urban morphology [16]. The concept of the UCM was first proposed by German scholars [17] and has been subsequently used in urban planning and local climate improvement [18]. Smith et al. found that a higher density of buildings and population exacerbated urban heat stresses [19]. Ren et al. analyzed the urban microclimate of Arnhem city using spatial data and found that land use was the most significant factor affecting the thermal load [20]. The UCM method is well suited to estimate the thermal environment of different regions according to the geographical characteristics and building characteristics in urban areas.

The optimization of the outdoor microclimate is affected by various climatic factors. The optimization of a single climatic factor may have adverse effects on other climatic factors. Therefore, the optimization of multiple climate factors has practical significance to improve the outdoor environment. Thus, the multiobjective optimization theory based on a genetic algorithm was used in this study, and we reviewed the literature on this topic [21]. Pareto proposed the Pareto solution set to describe the optimal state of resource allocation based on multiple objectives; the solution set is commonly depicted as a point distribution on a curve or surface [22]. The Pareto frontier can be solved using the strength Pareto evolutionary algorithm (SPEA) proposed by Zitzler [23]. A method of finding the Pareto optimal solution set was proposed by Wortmann et al. for use in architectural design [24]. Cui et al. established a microclimate optimization framework for the optimal design of an urban outdoor space in the cold regions in China [25]. Du et al. proposed a multistage optimization process to optimize the wind speed distribution and the thermal environment in urban canyons [26]. Waibel et al. presented a cosimulation framework for the optimization of building energy demand and solar potential [27].

The purpose of this study is to improve the outdoor microclimate on a university campus using campus layout design, which is achieved as follows:

(1) Morphological classification is used to describe the characteristics of university campuses in a cold region in China (Heilongjiang Province, Jilin Province, Liaoning Province) and develop a layout prototype of campus clusters

(2) The morphological characteristics of the campus are simplified, and a multiobjective optimization method combined with a genetic algorithm is used to conduct parametric linkage analysis and optimize the morphology

(3) According to the optimized solution set and the established quantitative equation, we suggest planning strategies for campus layouts to guide sustainable environmental planning on campuses

2. Methodology

2.1. Principle of Multiobjective Optimization. The influence on the outdoor microclimate differs for different spatial morphological parameters. For example, increasing the height (H) to width (W) ratio of streets can reduce the air temperature and solar radiation and improve the thermal environment in summer, but excessive wind speed will result in thermal discomfort [28]. In addition, a morphological layout that is suitable for the summer thermal environment may not have advantages in the winter [29]. In cases where different parameters have to be optimized simultaneously, Pareto optimization is commonly used. The Pareto optimal solution set, which is also known as the nondominated solution set, provides a balance of all optimization objectives. The distribution of nondominated solutions is called the Pareto frontier. The goal of multiobjective optimization is to determine the Pareto frontier. The mathematical description is as follows:

$$\begin{aligned} &\min f(x) = \left[f_1(x), f_2(x), \ldots f_p(x)\right]^T, \\ &\quad g_i(x) \geq 0, \quad i \in I, \\ &\quad h_j(x) = 0, \quad j \in E. \end{aligned} \tag{1}$$

As shown in equation (1), the variable feasible region is S and the corresponding target feasible region is $Z = f(S)$. For a viable solution $x^* \in S$, it should be $\forall x \in S$, $f(x'') \leq f(x)$, so x^* is the optimal solution for multiobjective optimization. If $x \in S$ does not exist which makes $f(x) < f(x')$, x^* is called an efficient solution, and x^* is the Pareto optimal solution of multiobjective programming.

2.2. Simulation-Based Optimization Workflow. For the design process, which generally uses simulation for performance prediction and optimization, the separation of the optimization and performance prediction processes often results in repetition and an increase in time cost. Thus, the simulation-based optimization workflow was established [30]. During the optimization process, some performance factors are often sacrificed to improve the performance of others, and the direction and effect of optimization are uncertain. The multiobjective optimization workflow allows for determining the complex competition among various performance factors and provides user-defined optimization [31].

The multiobjective optimization of the microclimate of the university campus cluster includes four steps, which are parametric modeling of the campus cluster, determination of the optimization objectives, calculation of the decision variables, and multiobjective optimization. We used a multiobjective optimization platform based on Rhinoceros and Grasshopper; the four steps are shown in Figure 1.

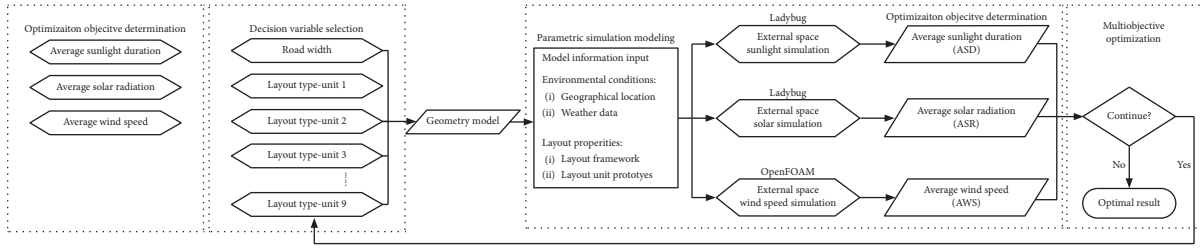

Figure 1: Simulation-based multiobjective optimization process.

(1) Determine the morphological parameters to be optimized based on the results of the morphology of the university campuses in the cold regions. Establish a cluster prototype parametric model that allows for the real-time adjustment of the parameters.

(2) Determine the optimization objectives according to the characteristics of the cold climate, such as the wind and thermal environment of the outdoor space.

(3) Select the decision variables according to the optimization objectives. The sunlight and solar radiation values of the outdoor space in the simulation were obtained using the Ladybug toolset [32]. The wind speed simulation was performed by importing the OpenFoam software [33] by the Butterfly toolset.

(4) Load the multiobjective evolutionary algorithm using the Octopus tool, link the optimization objective variables with the parameters of the campus cluster prototype, and generate a large number of optimized cluster prototype models for the multiobjective optimization.

2.3. The Morphological Characteristics of the Campus and Its Simplification. A survey of campuses in the cold region of China showed that the campuses consist of a teaching area, accommodation area, service area, and sports area, which are arranged in clusters. In this study, the clusters of 41 campuses were classified based on the layout and scale. It was found that the clusters consisted of several types of building types, including enclosed buildings, semienclosed buildings, and multistory buildings. A grid was used to analyze the pattern. The types of buildings and shape simplification are shown in Table 1. The survey data showed that the width of the streets on the campus was in the range of 5–20 m, the grid size ranged from 45 m to 100 m, and the area of the clusters ranged from 200 m × 200 m to 400 m × 400 m. The distance between the buildings in the East-West direction was 13–20 m, and that of the North-South direction ranged from 20 m to 30 m and depended on the height of the buildings. The building density of the campus cluster was 0.2–0.5, and the building plot ratio of the clusters was significantly different, ranging from 0.8 to 5. The number of stories of the buildings on the campus was in the range of 2–24, and most ranged from 4 to 12.

The types of buildings were simplified into nine types, with a size of 100 m × 100 m. The simplified model and corresponding parameters are shown in Table 2.

Based on the survey data and simplified building units, a cluster prototype of the campus was constructed; it consisted of nine 100 m × 100 m building units, and the street width ranged from 5 m to 20 m. The nine types of campus building units and open spaces were randomly distributed at the site, resulting in 9^{10} sets of clusters. Three cluster prototypes and the representative cases are shown in Table 3. The rapid generation of the cluster prototypes can be achieved by parametric modeling.

2.4. Optimization Objectives. Since this study focuses on adaptive planning of the campus layout in a severe cold climate, 41 university campuses were chosen in Northeast China (118°–135.2° E longitude, 38.7°–53.33°N latitude). The area has a temperate continental monsoon climate with long winters, low temperatures, and snow. The urban climate conditions in the severe cold region are shown in Table 4.

The objectives of this study were to maximize the sunlight duration and radiant heat gain of the outdoor space and minimize the wind speed to achieve the comfortable outdoor environment of the university campus. Three parameters were considered, namely, the average sunlight duration (ASLD), average solar radiation (ASR), and average wind speed (AWS). The optimization objectives are as follows:

ASLD: to increase the average sunlight hours in winter. The ASLD is the average value of sunlight hours on a cold day ($\hbar$) at the height of 0.9 m of the campus cluster; the unit is meter, and the values are obtained by simulation. The Octopus toolset calculates the minimum value of each objective value by default. The objective function of this parameter in the multiobjective optimization is α, $\alpha = -\hbar$.

ASR: to increase the radiant heat gain of the site during the heating period (10 : 20–16 : 20). The unit of the parameter is kW·H/m2, and the values are obtained by simulation. The objective function of this parameter in the optimization is γ, $\gamma = -\mathrm{I}$.

AWS: according to the characteristics of the Harbin urban wind field, the optimization objective is to decrease the average wind speed. The data are imported into the OpenFoam computing platform using the Butterfly toolset to simulate the wind speed distribution in the outdoor space of the cluster prototype. The prevailing wind direction in Harbin is WNW in winter, the initial wind speed is 5 m/s, the calculation grid size is 10 m × 10 m, and the wind speed is modeled at the height of 1.5 m. The objective function in the optimization is V.

Table 1: The layout of typical university campus clusters.

Northeastern University		Panjin Campus of Dalian University of Technology		Liaoning University	
		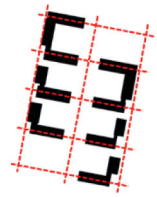		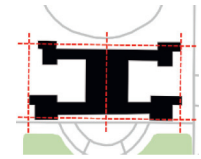	
Teaching cluster	Morphological simplification	Dormitory cluster	Morphological simplification	Teaching cluster	Morphological simplification
Enclosed		Semienclosed		Semienclosed	
Grid size: 70 m × 70 m Building depth: 16 m		Grid size: 60 m × 60 m Building depth: 14 m		Grid size: 55 m × 55 m Building depth: 11 m	
Harbin Institute of Technology		Northeast Normal University		Dalian University of Foreign Languages	
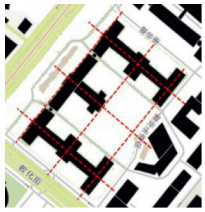		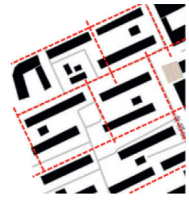	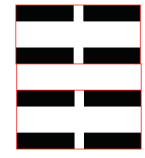	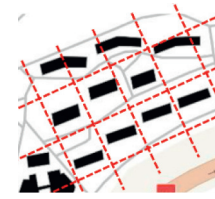	
Teaching cluster	Morphological simplification	Dormitory cluster	Morphological simplification	Dormitory cluster	Morphological simplification
Semienclosed		Determinant		Tower	
Grid size: 90 m × 60 m Building depth: 17 m		Grid size: 100 m × 90 m Building depth: 14 m		Grid size: 45 m × 45 m Building depth: 11 m	

2.5. Optimization Decision Variables and Constraints. The multiobjective optimization of the outdoor space microclimate of campus clusters is affected by various decision variables; the building density and plot ratio have the largest influences on the solar radiation of the outdoor space. The building height affects the solar radiation range and wind in the surrounding space, and the percentage of pavement area (PAVE) affects the ventilation performance of the external space. To simplify the optimization model, we focused on building morphology variables and cluster layout variables (Table 5).

2.5.1. Building Morphology Variables. After simplifying the types of campus buildings, nine types of buildings were extracted that cover different campus building types on university campuses in cold regions. The nine types of building modules were represented by 1–9, and 0 represented open spaces. In this manner, the layout types of different building types could be changed in the parametric module, as shown in Table 2, to create the layout of the campus cluster in the next step.

2.5.2. Cluster Layout Variables. The morphology of the university campus cluster is affected by many variables, such as the plane form, scale, and distance between buildings. Each of the nine 100 m × 100 m building areas could be assigned to 1 of the 9 building types in the parametric model to create different cluster morphologies. Thus, 910 sets of campus clusters were obtained. The building density ranged from 0 to 0.52, the plot ratio ranged from 0 to 5.62, and the width ranged from 6 m to 15 m, as shown in Table 5.

2.6. Parametric Simulation Modeling and Algorithm Settings. Based on the parametric modeling platforms Rhinoceros and Grasshopper, the campus cluster prototype model is integrated with the microclimate simulation of the outdoor space to establish a complete data flow and automatically generate the simulation model. In addition, Ladybug and Butterfly plugins were used to integrate the Grasshopper EnergyPlus Weather files (EPW), Dynamo, and OpenFoam. The optimization software platform is shown in Figure 2.

The EPW and Dynamo were used to calculate the sunlight duration and solar radiation, which allows for changing the simulation parameters, such as the building type and the road width of the cluster. The climate data of Harbin (45.77°N, 126.68°E), which is a typical city in the cold region of China, was chosen as the reference; the data were obtained from the EPW [29]. The location information was used to calculate the sunlight duration and the annual direct and scattered radiation values. The solar radiation data were imported into the simulation engine for the solar radiation calculation. The simulation-based optimization model is presented in Figure 3.

The optimization algorithm settings are listed in Table 6. Octopus provides two convergence mechanisms and three

Table 2: Simplified models of building units of campus clusters.

Type 1: multistory enclosed		Type 2: high-rising enclosed		Type 3: multistory semienclosed	
Building density	0.56	Building density	0.5	Building density	0.46
Plot ratio	2.8	Plot ratio	6	Plot ratio	2.3
Building levels	5	Building levels	12	Building levels	5
Type 4: high-rising semienclosed		Type 5: centralized (1)		Type 6: centralized (2)	
Building density	0.46	Building density	0.45	Building density	0.45
Plot ratio	5.5	Plot ratio	1.35	Plot ratio	1.35
Building levels	12	Building levels	3	Building levels	3
Type 7: multistory slab		Type 8: high-rising slab		Type 9: high-rising tower	
Building density	0.38	Building density	0.36	Building density	0.16
Plot ratio	2.3	Plot ratio	5.4	Plot ratio	3.8
Building levels	6	Building levels	12	Building levels	20

Table 3: The cluster prototypes and the representative campus cases.

Cluster prototypes			
	Building density 0.39 Plot ratio 3.24	Building density 0.35 Plot ratio 1.66	Building density 0.27 Plot ratio 2.72
Cases			
	Harbin Institute of Technology	Jilin Agricultural University	Dalian University of Foreign Languages

Table 4: Basic meteorological information of cities in cold region of China (2007–2017) [34].

	Daily maximum temperature (°C)	Daily minimum temperature (°C)	Mean temperature (°C)	RH (%)	Wind speed (km/h)	Sunshine duration (W/m^2)
Annual	10	−1.3	3.6	65	12	2571.2
Jan.	−13	−24	−19.4	72	17	155.9
Feb.	−7	−20	−15.4	68	16	179.9
Mar.	2	−10	−4.8	56	14	230.9
Apr.	13	1	6.0	49	9	231.4
May	21	8	14.3	51	9	264.1
Jun.	26	15	20.0	65	9	260.2
July	28	18	22.8	77	9	254.2
Aug.	26	16	21.1	78	12	247.2
Sept.	21	9	14.4	70	9	230.5
Oct.	12	1	5.6	63	8	206.8
Nov.	0	−10	−5.7	65	6	170.2
Dec.	−9	−20	−15.6	71	8	139.9

Table 5: The value ranges and the steps of decision variables.

Decision variables	Unit	Value ranges	Steps
Layout type-unit 1	—	0–9	1
Layout type-unit 2	—	0–9	1
Layout type-unit 3	—	0–9	1
Layout type-unit 4	—	0–9	1
Layout type-unit 5	—	0–9	1
Layout type-unit 6	—	0–9	1
Layout type-unit 7	—	0–9	1
Layout type-unit 8	—	0–9	1
Layout type-unit 9	—	0–9	1
Road width (W)	m	6–15	1

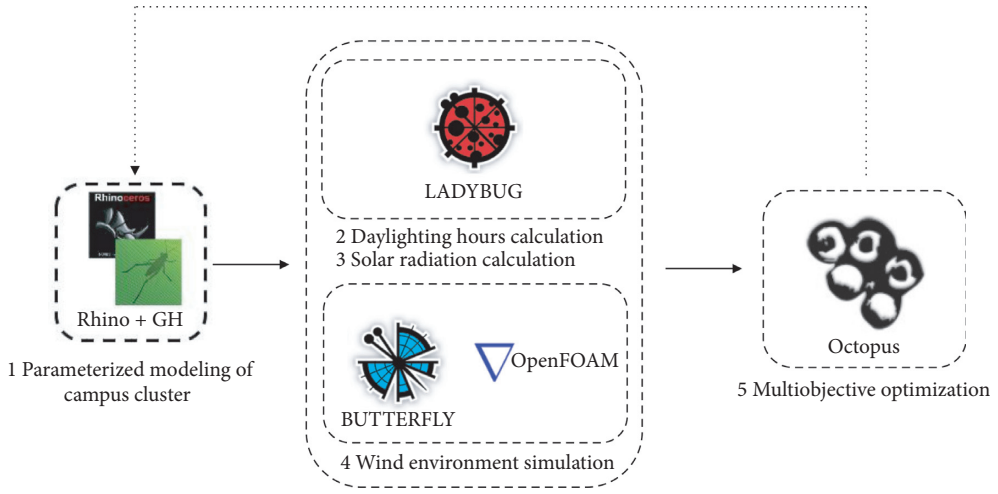

Figure 2: Toolsets of optimization program platform.

mutation mechanisms. The improved SPEA (SPEA-2) and polynomial mutation were used in the experiment to achieve good convergence and uniformity. The main parameter settings in octopus were elite ratio of 0.5, crossover probability of 0.8, mutation probability of 0.1, mutation ratio of 0.5, population size of 50, and maximum number of iterations of 40; the sunlight requirements were set as random constraints [35, 36].

3. Results and Discussion

3.1. Multiobjective Optimization of Campus Morphology. The multiobjective optimization calculation was performed for over 49 hr, and after 40 iterations, 108 nondominated solutions were obtained. As shown in Figure 4, the three axes represent the ASLD on cold days, the ASR during the heating period in winter, and the AWS of the outdoor

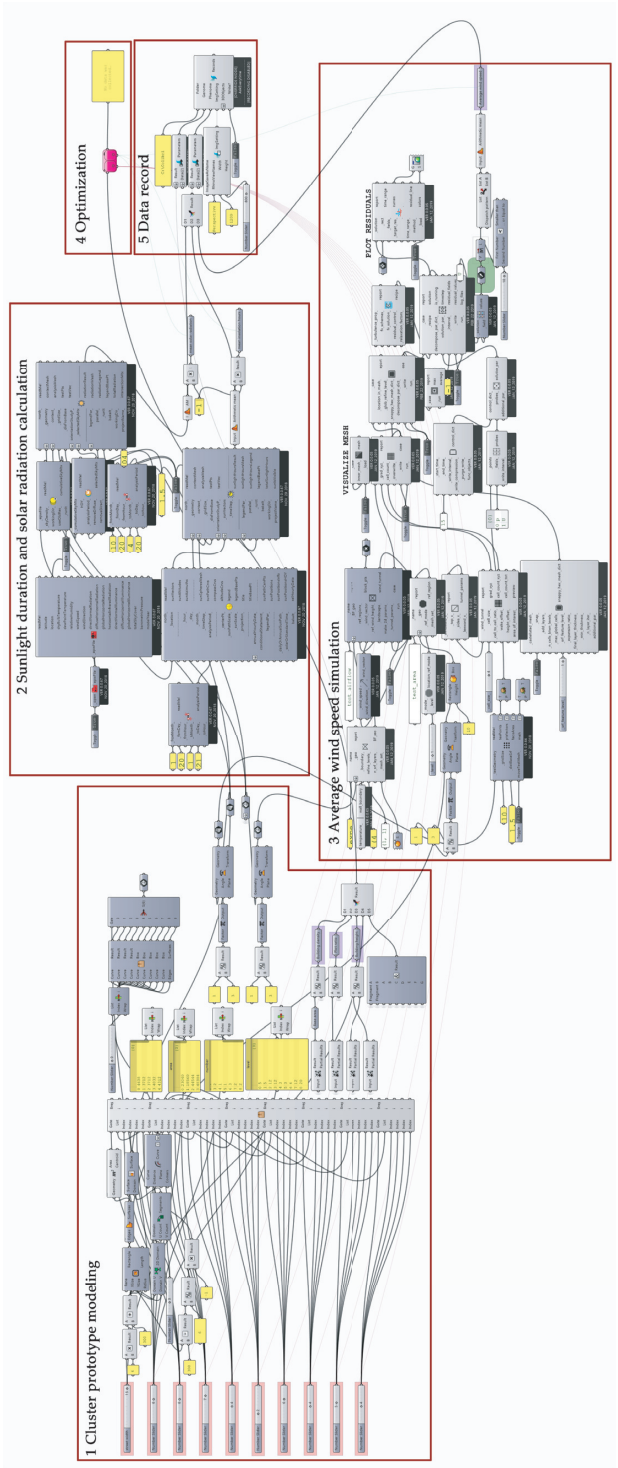

Figure 3: Simulation-based optimization model.

Table 6: Optimization algorithm settings [30].

Elitism	Mutation probability	Mutation rate	Crossover rate	Population size
0.50	0.10	0.50	0.80	50

space, respectively. Each point represents a group of solutions that correspond to a cluster prototype. The closer the objective values are to the origin, the better the solution performance is. The red-colored boxes represent the best performing solutions regarding the three optimization objectives.

As Figure 4(a) shows, each polygonal line represents a set of solutions, and the three objective values of ASLD, ASR, and AWS are mutually restricted. Figure 4(b) shows the Pareto front surface consisting of the nondominated solutions, and Figure 4(c) shows the distribution of the nondominated solutions in the coordinate system.

The spatial distribution of the nondominated solutions (Figure 5) indicates that the ASLD on cold days is positively correlated with the ASR in winter, and the relationship between the two parameters and the AWS is mutually restricted. The nondominated solutions of the ASLD range from 3.3 h to 8.07 h on cold days, and the ASR during the heating period ranges from 130.32 kW H/m2 to 235.74 kW H/m2. The AWS ranges from 1.76 m/s to 2.75 m/s (Figure 5).

Five typical cluster prototypes with nondominated solutions were analyzed (Table 7). Solution A has the optimal AWS, solution B has the optimal ASLD and ASR, and solutions *C*, *D*, and *E* are relatively balanced regarding the three optimization objectives. The optimization of the winter microclimate of the cluster can be achieved by changing the morphology parameters and the combination of multiple building units. Therefore, in the design, the morphological parameters should be considered to achieve a better microclimate.

3.2. Parameters of the Nondominated Solutions. The morphological parameters of the nondominated solutions were selected as the optimal value threshold (Figure 7). The building density was in the range of 0.17–0.31, and the median was 0.22. In half of the nondominated solutions, the building density was in the range of 0.21–0.23, indicating that more multiobjective optimization prototypes were obtained when using this value range as the building density of the cluster.

The plot ratio ranged from 0.99 to 2.51, and the median was 1.63. Most of the values were in the range of 1.51–1.88, which can be used as the reference range of the parameters for cluster morphology optimization.

The average number of stories of the buildings was in the range of 3–8.29, and the median was 5.34. Half of the values in the nondominated solutions were in the range of 4.63–6.14. The optimized average number of stories of the building was between 4 and 6.

The road width of the cluster prototype ranged from 6 m to 15 m, and the median was 14 m. Most of the values were in the range of 11 m–14 m; thus, this range is suggested as the optimum range of the road width.

When the parameters of the campus cluster are within these ranges, the cluster morphology is optimized regarding the ASLD, ASR, and AWS in winter, and the microclimate of the outdoor space is optimized.

The building density (Figure 8) and road width (Figure 9) of the nondominated solution were proportional to the ASLD and ASR and inversely proportional to the AWS. The plot ratio (Figure 10) and the average number of stories (Figure 11) of the nondominated solution were inversely proportional to the ASLD and ASR and proportional to the AWS (Figure 10).

3.3. Recommendations Based on the Parameters of the Nondominated Solutions. According to the parametric analysis of the nondominated solutions, the optimal range of the building density is 0.21–0.23, and the types of qualified buildings include the following:

(1) Type 7: multistory building (building density: 0.38)

(2) Type 8: high-rise building (building density: 0.36)

(3) Type 9: high-rise tower (building density: 0.16)

The optimal range of the plot ratio is 1.51–1.88, and the types of qualified buildings include the following:

(1) Type 3: multistory semienclosed (plot ratio: 2.3)

(2) Type 5: centralized (1) (plot ratio: 1.35)

(3) Type 6: centralized (2) (plot ratio: 1.35)

(4) Type 7: multistory building (plot ratio: 2.3), which can be used as the preferred building form (Table 2)

The simulation results of the optimal solutions showed higher wind speeds near the high-rise buildings; thus, multistory buildings should represent the main component of the campus cluster, such as type 7. The enclosed and semienclosed layout resulted in lower wind speeds of the outdoor space; when the longitudinal direction of the building was the same as the wind direction, the wind speed of the enclosed space was significantly reduced.

In the climate conditions of Harbin, the open spaces in the southeast of the campus provided advantages regarding sunlight and solar radiation, and the sunlight duration could be increased by increasing the building spacing. It is suggested to optimize the microclimate of the outdoor space by maintaining the average number of stories at 3–8.3 and the road width at 11–14 m. Green vegetation can be used to change the roughness of the surface to optimize the outdoor wind speed in winter.

3.4. Comparison of the Conditions before and after Multiobjective Optimization

3.4.1. Before Optimization. A model of Jilin Agricultural University was established using the Rhinoceros and Grasshopper platforms, and a simulation was performed with three optimization objectives: ASLD, ASR, and AWS. The results are shown in Figure 12.

Figure 12(a) shows the key points in the cluster space that were quantitatively analyzed. The sunlight duration of the cluster model on cold days was calculated using the Ladybug tool set. The ASLD was 0 to 18 h, with a mean value of 5.56 h. Figure 12(b) shows that the ASLD was low; 80% of the open space had an ASLD of 0 h to 7.2 h, and at the

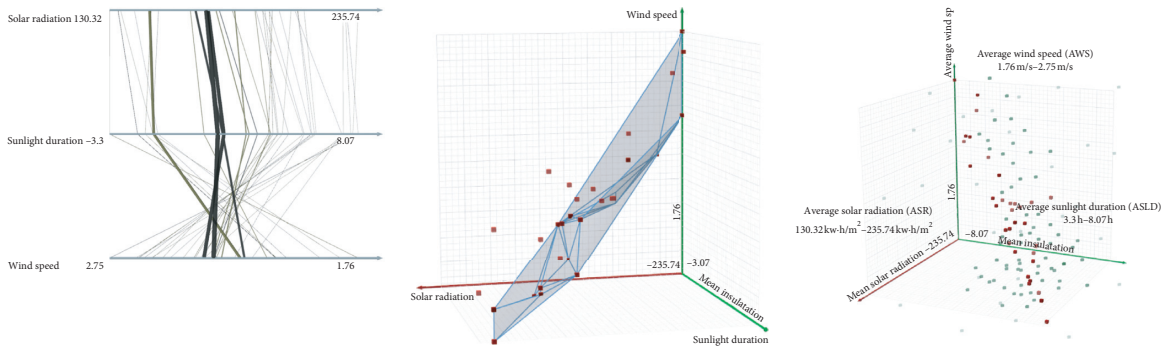

(a) (b) (c)

Figure 4: Distribution of multiobjective optimization solutions. (a) Multiaxe view of nondominated solutions. (b) Delaunay of Pareto front. (c) Distribution of Pareto solutions.

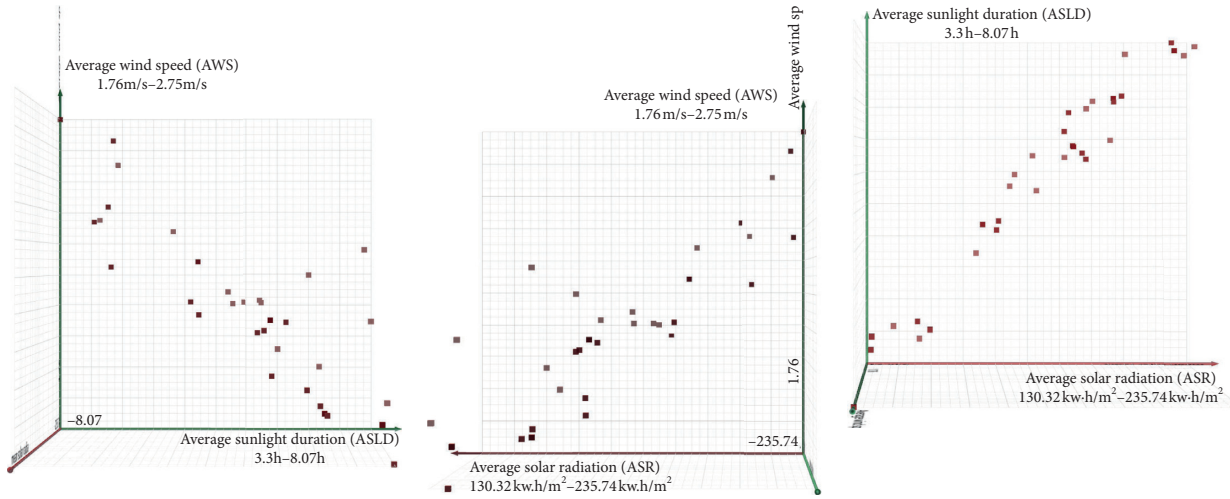

(a) (b) (c)

Figure 5: Distribution of nondominated solutions. (a) Average wind speed and average sunlight duration. (b) Average wind speed and average solar radiation. (c) Average sunlight duration and average solar radiation.

locations ③ and ④, the ASLD was close to 0 h. At ①, ②, and ⑥, the ASLD was between 0 h and 1.8 h. The data shows that the outdoor environment of the cluster requires improvement in terms of sunlight duration.

The ASR in winter ranged from 0 kW H/m^2 to 357.6 kW H/m^2, with a mean value of 162.58 kW H/m^2. Figure 12(c) shows that at points ④ and ⑤, the ASR was near the minimum area, which was between 0 kW H/m^2 and 143.0 kW H/m^2. There was a greater distance between the buildings in the North-South direction, and the maximum value of the ASR was 321.84 kW H/m^2. The distribution of the solar radiation in the cluster space was uneven, resulting in differences in the heat gain of the cluster space; this aspect requires further improvement.

The Butterfly toolset was used to simulate the wind environment of the cluster space. The initial wind speed was 5 m/s, and the dominant wind direction in winter is WSW. Figure 12(d) shows that the AWS in the cluster space is between 0 m/s and 4 m/s, with a mean value of 1.99 m/s. At points ⑦ and ⑧, the AWS was in the range of 0.58 m/s −2.48 m/s, representing the area with the lowest wind speed in the cluster space. At ①, ③, ④, and ⑤, the wind speed was higher, especially near the edge of the buildings, and reached 4 m/s, which substantially decreased the thermal comfort of the outdoor space in winter. It is necessary to adjust the morphology of the cluster and optimize the local wind environment.

3.4.2. After Optimization. The proposed design recommendations for Jilin Agricultural University take into account that the sunlight duration is short, such as at ③, ④, and ⑤, where high wind speeds of above 4 m/s were observed. The layout of the three centralized buildings in the cluster was adjusted, as shown in Figure 13(a). First, the distance between the buildings was changed from 6 m to 12 m, which increased the building spacing and the sunlight duration, as shown in Figure 13(b). Points ③, ④, and ⑤ were well optimized, and the solar radiation was also well

Table 7: Typical cluster prototypes corresponding to the nondominated solutions.

Objectives	Average sunlight duration ($\hbar$)	Average solar radiation (I)	Average wind speed (V)	Cluster prototype morphology
A $\hbar = 5.40$ h $I = 184.20$ kW H/m^2 $\overline{v} = 1.86$ m/s	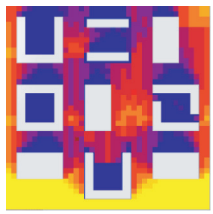	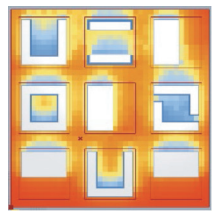	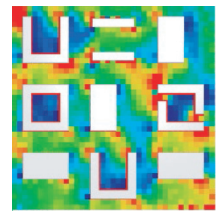	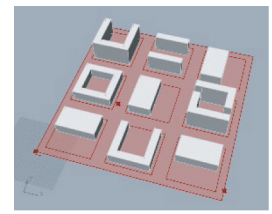
B $\hbar = 8.07$ h $I = 235.75$ kW H/m^2 $\overline{v} = 2.73$ m/s	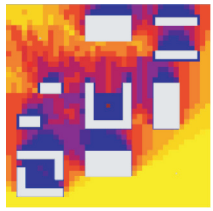	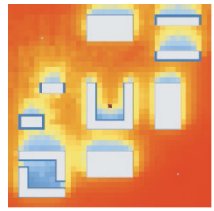	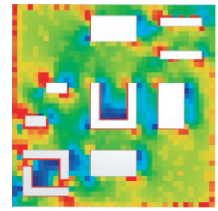	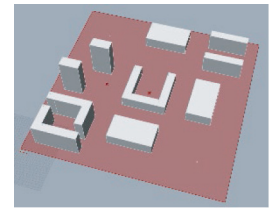
C $\hbar = 6.09$ h $I = 203.73$ kW H/m^2 $\overline{v} = 2.11$ m/s	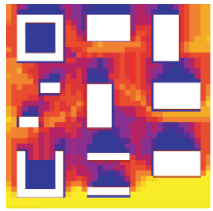	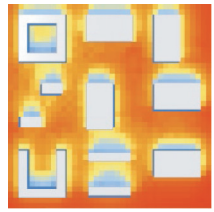	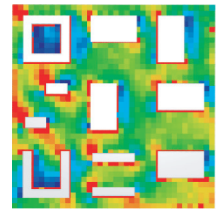	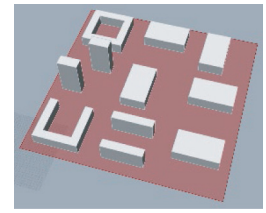
D $\hbar = 6.76$ h $I = 205.80$ kW H/m^2 $\overline{v} = 2.60$ m/s		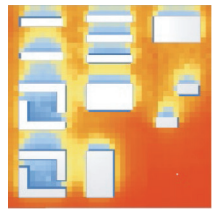	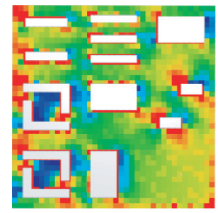	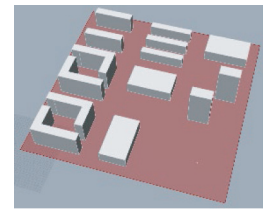
E $\hbar = 6.20$ h $I = 201.77$ kW H/m^2 $\overline{v} = 1.97$ m/s	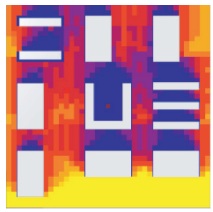	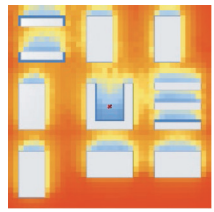	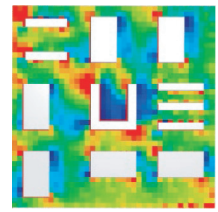	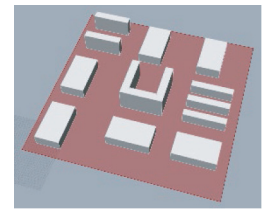

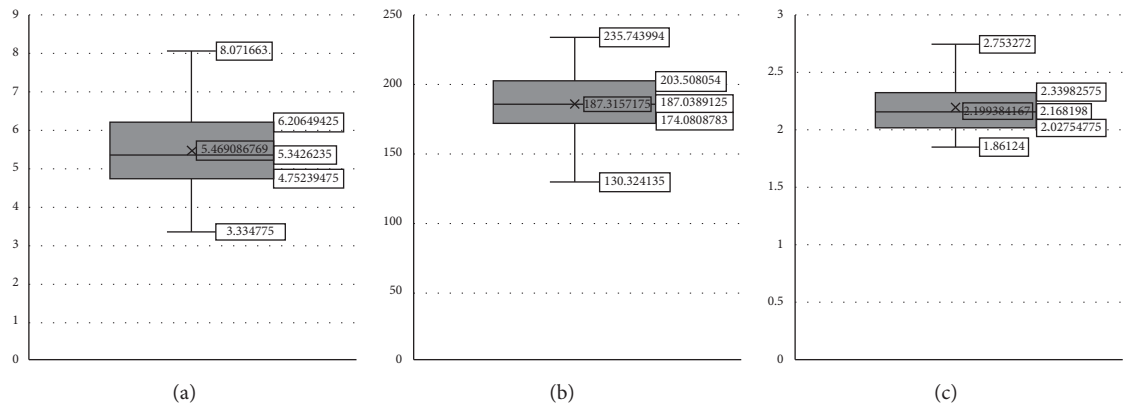

Figure 6: Numerical distribution of the optimization objectives. (a) Average sunlight duration ($\hbar$). (b) Average solar radiation (I). (c) Average wind speed (V).

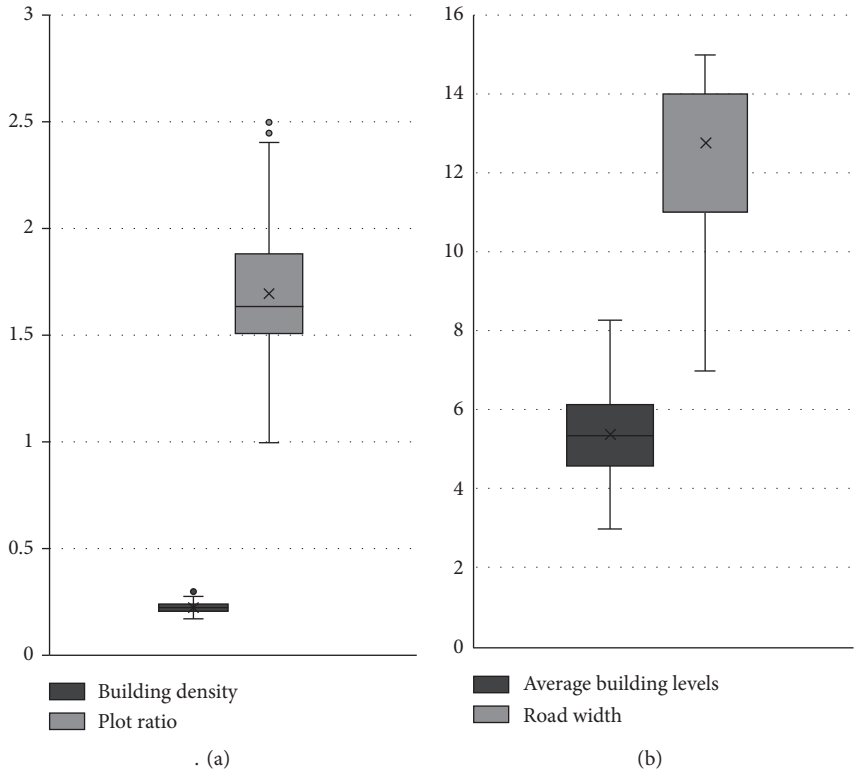

Figure 7: Parameters distribution of the nondominated solutions. (a) Building density and plot ratio. (b) Average building levels and road width.

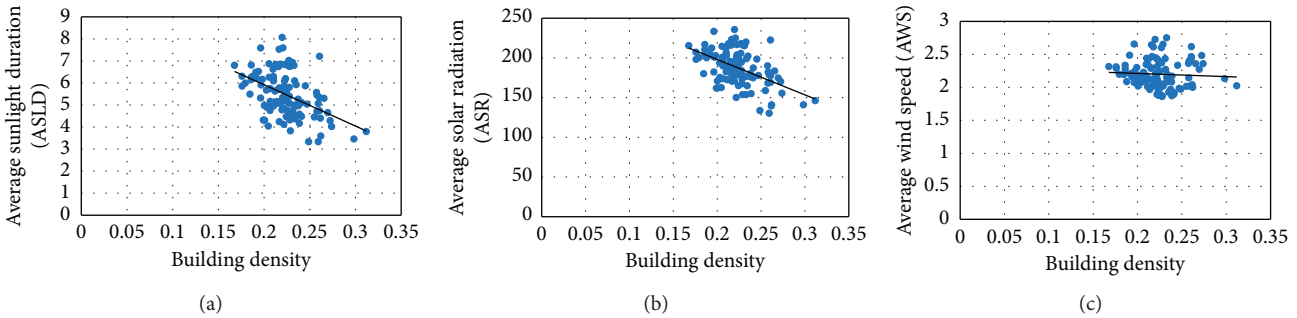

Figure 8: Relationship between building density of the nondominated solutions and objectives. (a) Building density and ASLD. (b) Building density and ASR. (c) Building density and AWS.

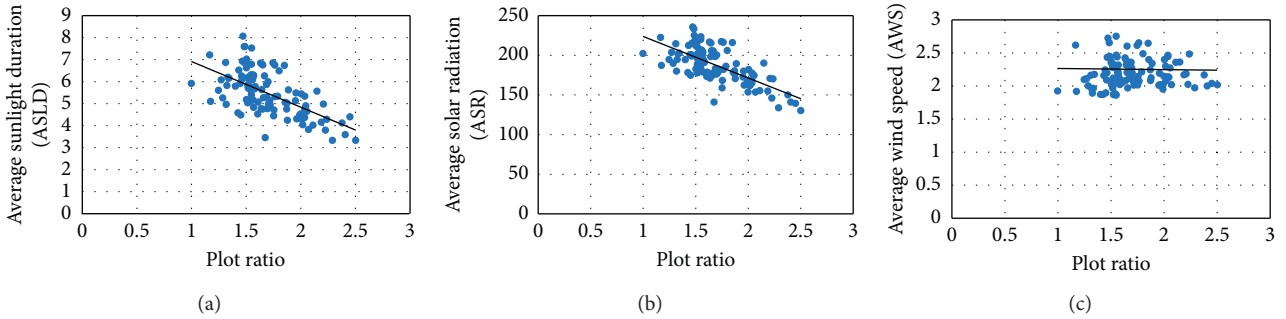

Figure 9: Relationship between road width of the nondominated solutions and objectives. (a) Road width and ASLD. (b) Road width and ASR. (c) Road width and AWS.

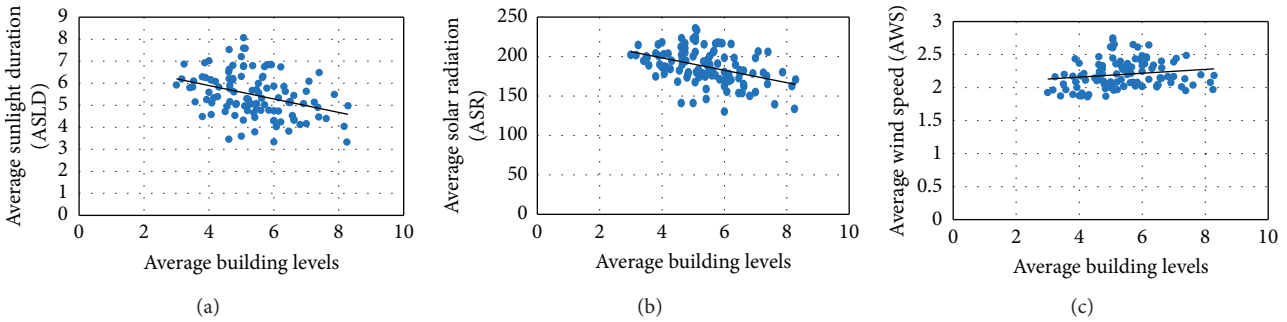

(a) (b) (c)

Figure 10: Relationship between plot ratio of the nondominated solutions and objectives. (a) Plot ratio and ASLD. (b) Plot ratio and ASR. (c) Plot ratio and AWS.

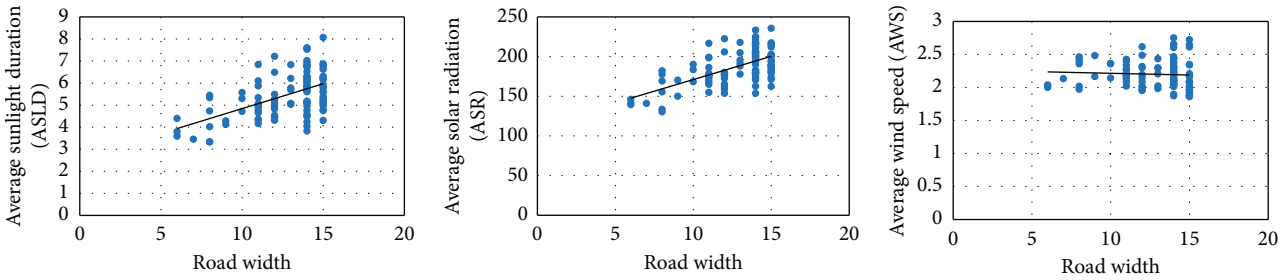

(a) (b) (c)

Figure 11: Relationship between average building levels of the nondominated solutions and objectives. (a) Average building levels and ASLD. (b) Average building levels and ASR. (c) Average building levels and AWS.

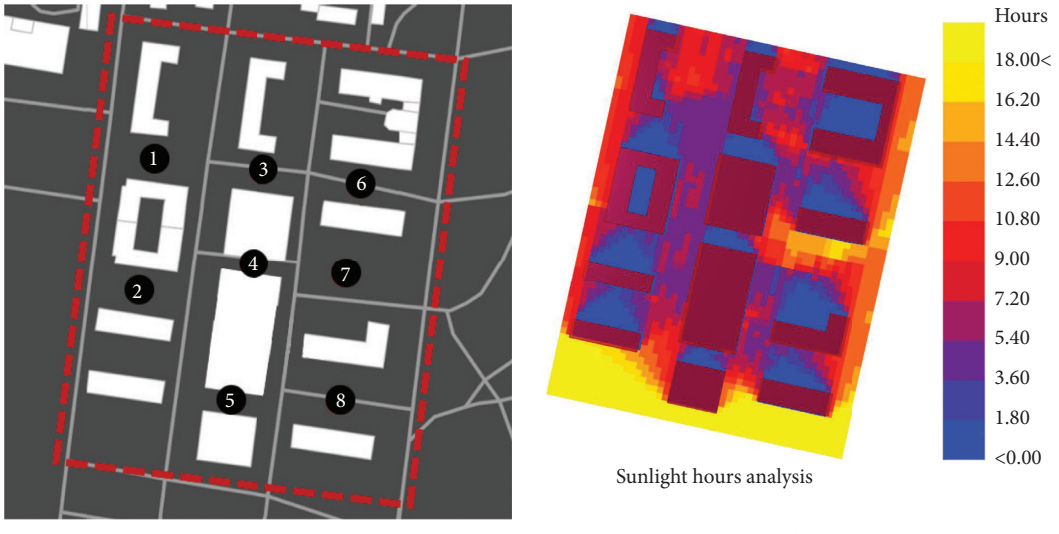

(a) (b)

Figure 12: Continued.

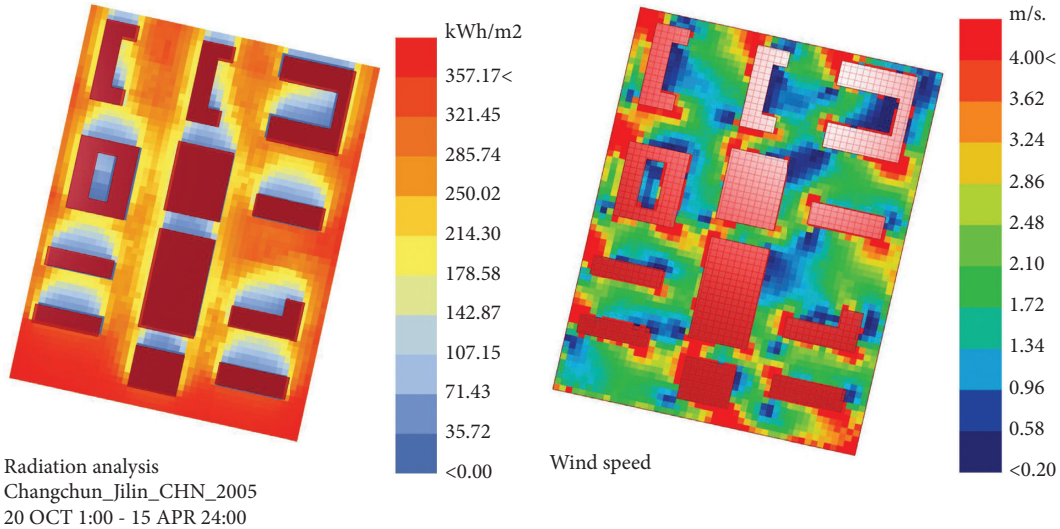

(c) (d)

Figure 12: Cluster space modeling of Jilin Agricultural University. (a) Key points distribution. (b) Distribution of sunlight duration on cold days. (c) Distribution of solar radiation in winter (10.20–4.15). (d) Wind speed distribution in the external space of the cluster affected by the dominant wind direction in winter.

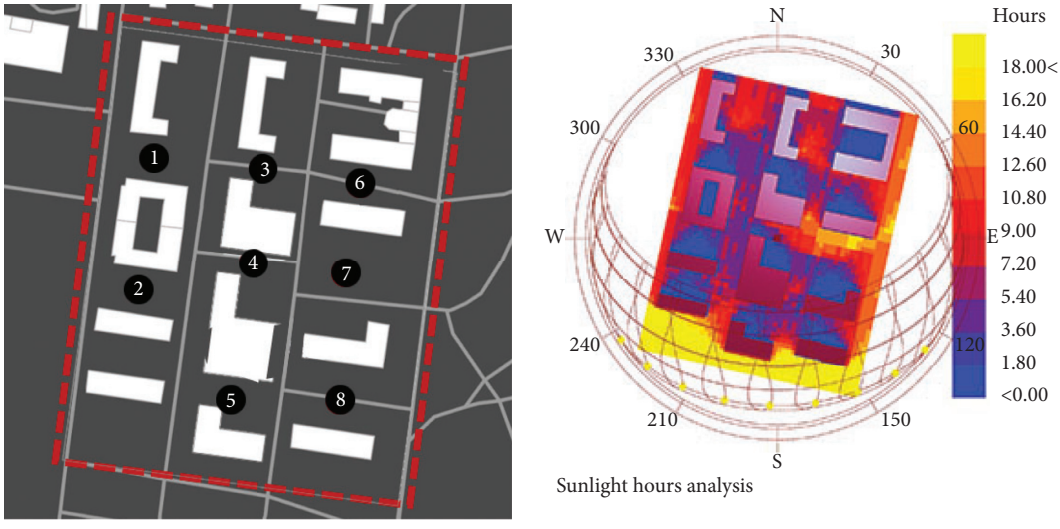

. (a) (b)

Figure 13: Continued.

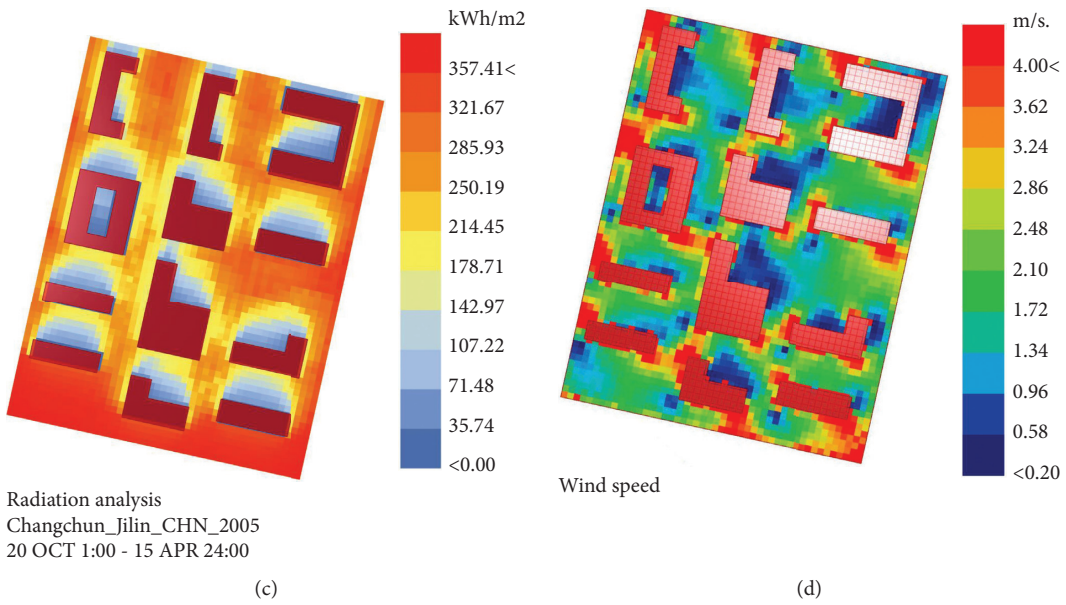

Figure 13: Cluster space optimal modeling of Jilin Agricultural University. (a) Key points distribution. (b) Distribution of sunlight duration on cold days. (c) Distribution of solar radiation in winter (10.20–4.15). (d) Wind speed distribution in the external space of the cluster affected by the dominant wind direction in winter.

optimized, as shown in Figure 13(c). Second, we adjusted the building form to an L-shape according to the wind direction to block the cold wind in winter, as shown in Figure 13(d). Since the average number of stories of the original building cluster was 5, which is within the optimal value range, the building height was not changed. In addition, the optimal sunlight duration of the outdoor space after optimization was 5.59 h, the sunshine radiation was 166.94 kW H/m^2, and the AWS was 1.94 m/s. The optimized cluster morphology resulted in an improved microclimate, demonstrating the excellent performance of the optimization model. Moreover, the passage space was changed to a square space that provides a positive public outdoor space on campus.

4. Conclusions

In this study, 41 university campuses in three northeastern provinces of China were surveyed, and the morphology was simplified. A prototype of the campus cluster was created with 9 types of building units, and the parametric model was established using the Rhinoceros and Grasshopper modeling method. Different building types and road widths were modeled, resulting in different building densities, plot ratios, and the average number of stories.

Three optimization objectives were used to optimize the outdoor microclimate of the campus cluster in winter, namely, maximizing the ASLD on cold days and the ASR during the heating period and minimizing the AWS. A parameterized platform was established for the optimization using the morphological parameters of the cluster prototype. The SPEA-2 was used for the multiobjective optimization, and 108 sets of nondominated solutions were obtained.

The ASLD of the open space on cold days ranged from 3.3 h to 8.07 h, the ASR was in the range of 130.32 kW H/m^2–235.7 kW H/m^2, and the AWS was 1.76 m/s–2.75 m/s. After multiobjective optimization of the three parameters, the building density of the cluster was 0.21–0.23, the plot ratio was 1.51–1.88, the average number of stories of the buildings was 4–6, and the street width was 11–14 m to achieve the optimum microclimate of the prototype of the campus cluster. Our design recommendations based on the optimization of the Jilin Agricultural University campus are as follows: the building shape should match the wind direction in winter, the space between buildings should be increased, the average number of stories should be 3–8.3, and the road width should be 11–14 m.

In the optimization of the campus outdoor space environment of Cold Regions University, there are many factors that have not been discussed in this study, such as orientation, vegetation, and vision, which will continue to be paid attention to in the future research.

Data Availability

The data used to support the findings of this study are available from the corresponding author upon request.

Conflicts of Interest

The authors declare that they have no conflicts of interest.

Acknowledgments

The authors wish to thank members of the Architecture Creation Research Institute for the support of this work. This research was financially supported by the Beijing Postdoctoral Research Foundation (Contract no. 2021-ZZ-107) and National Natural Science Foundation of China (no. 51778008).

References

[1] D. G. Özkan, E. M. Alpak, and M. Var, "Design and construction process in campus open spaces: a case study of Karadeniz Technical University," *Urban Design International*, vol. 22, no. 3, pp. 236–252, 2017.

[2] A. Ghaffarianhoseini, U. Berardi, A. Ghaffarianhoseini, and K. Al-Obaidi, "Analyzing the thermal comfort conditions of outdoor spaces in a university campus in Kuala Lumpur, Malaysia," *Science of the Total Environment*, vol. 666, pp. 1327–1345, 2019.

[3] Y. Wang, R. De Groot, F. Bakker, H. Wörtche, and R. Leemans, "Thermal comfort in urban green spaces: a survey on a Dutch university campus," *International Journal of Biometeorology*, vol. 61, no. 1, pp. 87–101, 2017.

[4] F. Salata, I. Golasi, D. Petitti, E. De Lieto Vollaro, M. Coppi, and A. De Lieto Vollaro, "Relating microclimate, human thermal comfort and health during heat waves: an analysis of heat island mitigation strategies through a case study in an urban outdoor environment," *Sustainable Cities and Society*, vol. 30, pp. 79–96, 2017.

[5] H. Jin, P. Cui, N. Wong, and M. Ignatius, "Assessing the effects of urban morphology parameters on microclimate in Singapore to control the urban heat island effect," *Sustainability*, vol. 10, no. 1, p. 206, 2018.

[6] M. Huang, P. Cui, and X. He, "Study of the cooling effects of urban green space in Harbin in terms of reducing the heat island effect," *Sustainability*, vol. 10, p. 1101, 2018.

[7] P. T. Nastos, K. P. Moustris, I. Charalampopoulos, I. K. Larissi, and A. G. Paliatsos, "Assessment of the thermal comfort conditions in a university campus using a 3D microscale climate model utilizing mobile measurements," in *Proceedings of the 13th International Conference on Meteorology Climatology and Atmospheric Physics (COMECAP)*, Thessaloniki, Greece, September 2016.

[8] T. S. Karacostas, A. F. Bais, and P. T. Nastos, *Perspectives on Atmospheric Sciences*, Springer International Publishing, Berlin, Germany, 2017.

[9] M. Taleghani, L. Kleerekoper, M. Tenpierik, and A. Van Den Dobbelsteen, "Outdoor thermal comfort within five different urban forms in The Netherlands," *Building and Environment*, vol. 83, pp. 65–78, 2015.

[10] X. Xie, O. Sahin, Z. Luo, and R. Yao, "Impact of neighbourhood-scale climate characteristics on building heating demand and night ventilation cooling potential," *Renewable Energy*, vol. 150, pp. 943–956, 2020.

[11] T. Huang, J. N. Li, Y. X. Xie et al., "Simultaneous environmental parameter monitoring and human subject survey regarding outdoor thermal comfort and its modelling," *Building and Environment*, vol. 125, pp. 502–514, 2017.

[12] A. Zhang, R. Bokel, A. Van Den Dobbelsteen, Y. Sun, Q. Huang, and Q. Zhang, "An integrated school and schoolyard design method for summer thermal comfort and energy efficiency in Northern China," *Building and Environment*, vol. 124, pp. 369–387, 2017.

[13] A. Battisti, F. Laureti, M. Zinzi, and G. Volpicelli, "Climate mitigation and adaptation strategies for roofs and pavements: a case study at sapienza university campus," *Sustainability*, vol. 10, no. 10, p. 3788, 2018.

[14] Q. J. Xu, Y. H. Ju, and H. H. Ge, "Field measurement and analysis of the micro climate of a campus square," *Advanced Materials Research*, pp. 610–613, 2013.

[15] S. A. Zaki, N. E. Othman, S. W. Syahidah et al., "Effects of urban morphology on microclimate parameters in an urban university campus," *Sustainability*, vol. 12, no. 7, p. 2962, 2020.

[16] X. He, S. Shen, S. Miao, J. Dou, and Y. Zhang, "Quantitative detection of urban climate resources and the establishment of an urban climate map (UCMap) system in Beijing," *Building and Environment*, vol. 92, pp. 668–678, 2015.

[17] C. Ren, E. Y.-y. Ng, and L. Katzschner, "Urban climatic map studies: a review," *International Journal Of Climatology*, vol. 31, no. 15, pp. 2213–2233, 2011.

[18] J. Unger, "Intra-urban relationship between surface geometry and urban heat island: review and new approach," *Climate Research*, vol. 27, pp. 253–264, 2004.

[19] C. Smith, S. Lindley, and G. Levermore, "Estimating spatial and temporal patterns of urban anthropogenic heat fluxes for UK cities: the case of Manchester," *Theoretical and Applied Climatology*, vol. 98, no. 1-2, pp. 19–35, 2009.

[20] C. Ren, T. Spit, S. Lenzholzer et al., "Urban climate map system for Dutch spatial planning," *International Journal of Applied Earth Observation and Geoinformation*, vol. 18, pp. 207–221, 2012.

[21] S. Yeung and K. Man, "Multiobjective optimization," *IEEE Microwave Magazine*, vol. 12, no. 6, pp. 120–133, 2011.

[22] I. Costa-Carrapico, R. Raslan, and J. N. Gonzalez, "A systematic review of genetic algorithm-based multi-objective optimisation for building retrofitting strategies towards energy efficiency," *Building and Environment*, vol. 210, 2020.

[23] E. Zitzler and L. Thiele, "Multiobjective evolutionary algorithms: a comparative case study and the strength Pareto approach," *IEEE Transactions on Evolutionary Computation*, vol. 3, no. 4, pp. 257–271, 1999.

[24] T. Wortmann and G. Nannicini, "Introduction to architectural design optimization," *City Networks*, vol. 259-278, pp. 259–278, 2017.

[25] J. Zhang, P. Cui, and H. H. Song, "Impact of urban morphology on outdoor air temperature and microclimate optimization strategy base on Pareto optimality in Northeast China," *Building and Environment*, 2020, in press.

[26] Y. Du, C. M. Mak, and Y. Li, "A multi-stage optimization of pedestrian level wind environment and thermal comfort with lift-up design in ideal urban canyons," *Sustainable Cities and Society*, vol. 46, p. 101424, 2019.

[27] C. Waibel, R. Evins, and J. Carmeliet, "Co-simulation and optimization of building geometry and multi-energy systems: interdependencies in energy supply, energy demand and solar potentials," *Applied Energy*, vol. 242, pp. 1661–1682, 2019.

[28] X. Xu, Y. Liu, W. Wang, N. Xu, K. Liu, and G. Yu, "Urban layout optimization based on genetic algorithm for microclimate performance in the cold region of China," *Applied Sciences*, vol. 9, no. 22, p. 4747, 2019.

[29] X. Xu, Y. Wu, W. Wang, T. Hong, and N. Xu, "Performance-driven optimization of urban open space configuration in the cold-winter and hot-summer region of China," *Building Simulation*, vol. 12, no. 3, pp. 411–424, 2019.

[30] Y. Han, H. Yu, and C. Sun, "Simulation-based multiobjective optimization of timber-glass residential buildings in severe cold regions," *Sustainability*, vol. 9, no. 12, p. 2353, 2017.

[31] N. Srinivas and K. Deb, "Muiltiobjective optimization using nondominated sorting in genetic algorithms," *Evolutionary Computation*, vol. 2, no. 3, pp. 221–248, 1994.

[32] M. S. Roudsari and M. Pak, "Ladybug: a parametric environmental plugin for grasshopper to help designers create an environmentally-conscious design," in *Proceedings of the 13th Conference of international Building Performance Simulation Association*, Chembery, France, August, 2013.

[33] H. Jasak, "OpenFOAM: open source CFD in research and industry," *International Journal of Naval Architecture and Ocean Engineering*, vol. 1, no. 2, pp. 89–94, 2009.
[34] H. Jin, L. Qiao, and P. Cui, "Study on the effect of streets' space forms on campus microclimate in the severe cold region of China-case study of a university campus in daqing city," *International Journal of Environmental Research and Public Health*, vol. 17, no. 22, p. 8389, 2020.
[35] U.S. Department of Energy, "Auxiliary programs," 2017, https://energyplus.net/.
[36] J. Bade and E. Zitzler, "An algorithm for fast hypervolume-based many-objective optimization," *Evol.Comput*, vol. 19, pp. 45–76, 2014.